ELSEVIER

Thermochimica Acta 364 (2000) 193–201

thermochimica acta

www.elsevier.com/locate/tca

Hofmann degradation kinetics of *n*-octylamine adsorbed on layered aluminosilicates prepared from apophyllite

Yu Sogo[a,*], Tsutomu Kumazawa[b], Ken Okihara[b], Atsushi Yamazaki[b]

[a]*National Institute for Advanced Interdisciplinary Research, 1-1-4 Higashi, Tsukuba-shi, Ibaraki 305-8562, Japan*
[b]*Department of Resources and Environmental Engineering, Waseda University, 3-4-1 Ohkubo, Shinjuku-ku, Tokyo 169-8555, Japan*

Received 11 April 2000; received in revised form 7 August 2000; accepted 20 August 2000

Abstract

Kinetic analyses of the Hofmann degradation of *n*-octylamine adsorbed on layered aluminosilicates prepared from apophyllite are reported. The data were collected by simultaneous thermogravimetry and evolved gas analysis (TG-DTG-EGA). Based on Kissinger plots using the DTG data, it is indicated that the activation energy of the Hofmann degradation increases with increasing Al/Si ratio of the layered aluminosilicates. Using the EGA data for 1-octene, a similar tendency is observed. However, there is no such tendency for the results using the EGA data for ammonia. This indicates that ammonia remain on the surface after the Hofmann degradation. Hence, the activation energy obtained for ammonia is not that of the *n*-octylamine decomposition, but from the analyses, using Ozawa's method, no tendency is observed in the relationship between the activation energy and the Al/Si ratio of the samples. This indicates that the Hofmann degradation is not a single elementary reaction in the strict meaning. However, the reaction mechanism could be estimated; e.g. two-dimensional dispersion (D2) for the sample with an Al/Si ratio in the range of 0.13−0.18 and three-dimensional dispersion (D4) for the Al/Si ratio of 0.05−0.09.

Keywords: Hofmann degradation; Apophyllite; Layered aluminosilicate; Kinetic analysis; TG-DTA-EGA

1. Introduction

Apophyllite is one of the phyllosilicate minerals, which consists of unique silicate sheets. Previously, it was shown that several kinds of layered silicates [1,2] and layered aluminosilicates [3] can be prepared from apophyllite. It was also found that the Al/Si ratio of these samples depends on the concentration of the reaction solution during the preparation. In the structure of these samples, the SiO_4 sheet structure of apophyllite is basically maintained. Due to their unique structures, it is presumed that these aluminosilicate samples should have some characteristic properties, e.g. an acidic property.

The acidic properties of the solid catalytic samples are generally examined by infrared spectrometry using organic bases, for example, pyridine and amine, as probe molecules [4–9]. Thermal analysis is also one of the useful tools for estimating the acidity of catalytic materials [10–13]. Especially, temperature-programmed desorption is used to characterize surface acid sites on solid acid catalysts, e.g. various kinds of zeolites [14]. From studies on the desorption of basic molecules from aluminosilicate samples, it is known that amine molecules adsorbed on Brønsted sites decompose alkene and ammonia by the Hofmann

* Corresponding author. Fax: +81-298-61-2565.
E-mail address: yusogo@nair.go.jp (Y. Sogo).

0040-6031/00/$ – see front matter
PII: S0040-6031(00)00643-2

degradation mechanism during heating [10,11]. The same reaction is also observed for *n*-octylamine intercalated in the layered aluminosilicate samples prepared from apophyllite [15]. However, there is little information about the decomposition process of amine molecules adsorbed on aluminosilicate samples, especially for layered samples. Furthermore, the acidity of the samples should have some relationship with their aluminum contents [7]. This means that the decomposition process of the intercalated amine molecule is dependent on the aluminum content of the samples. It is important to examine the acid properties of the layered aluminosilicates from natural minerals because it will determine the possible use of these minerals in industry.

In this study, the thermal decomposition data of *n*-octylamine intercalated into the aluminosilicate samples obtained from apophyllite were recorded at constant heating rates. The Hofmann degradation of the samples was analyzed and the catalytic properties of the aluminosilicates were considered.

2. Experimental

2.1. Sample preparation

Apophyllite from Jalgaon, Maharashtra, India, was used as the starting material. According to the chemical analysis, the chemical composition of this apophyllite sample was determined to be $(K_{1.04}, Na_{0.03})$ $Ca_{4.02}$ $(Si_{7.72}, Al_{0.01})$ O_{20} (F, OH)·$6.75H_2O$. This composition corresponds to the ideal formula of apophyllite.

Five kinds of layered aluminosilicates were prepared from apophyllite as follows. A 250 mg sample of natural apophyllite powder ground to less than 75 μm was dispersed in 50 cm^3 of aluminum chloride solution. The concentration of the reaction solution was varied between 0.05 and 1.00 mol dm^{-3}. This suspension was stirred using a magnetic stirrer at room temperature for a period of 10–15 days. The solid phase was then centrifugally separated (15 min at 3000 rpm). The separated solid phase was washed three times by distilled water. Finally, this solid phase was dried at ca. 10°C for 1 day and the particle size of these products was adjusted to <75 μm again. These samples were labeled Al-AP.

Table 1
Conditions of sample preparation and the Al/Si ratio of the resulting samples

Sample name	$AlCl_3$ solution treatment		Al/Si ratio
	Concentration (mol dm^{-3})	Duration (day)	
Al-AP-100	1.00	10	0.18
Al-AP-050	0.50	10	0.17
Al-AP-020	0.20	10	0.13
Al-AP-010	0.10	10	0.09
Al-AP-005	0.05	15	0.05

The preparation conditions of all the Al-AP samples are listed in Table 1. Under these conditions, samples with an Al/Si ratio of 0.05−0.18 were obtained. The Al-AP samples are described as Al-AP-*X*, where *X* represents the concentration of the reaction solution used in sample preparation. For example, Al-AP-010 was prepared with 0.10 mol dm^{-3} of aluminum chloride solution.

N-octylamine (hereafter abbreviated as *n*-OA) is then intercalated into the Al-AP samples in the following way: 200 mg of the sample was dispersed in *n*-OA solution, which is a mixture of 2 ml of *n*-OA and 10 ml of methanol. This suspension was allowed to stand for 1 day. The solid phase was then separated from the liquid phase by centrifugation (15 min, 3000 rpm). The solid phase was then dried at room temperature. From the XRD patterns of the samples after the *n*-OA treatment, the *n*-OA intercalated to interlayer space of Al-AP samples was determined.

2.2. Methods

The chemical compositions of the Al-AP samples were analyzed by energy dispersive spectroscopy (EDS) using a Link QX 200J attached to a JEOL JSM-5400 with an accelerating voltage at 15 kV. Simultaneous thermogravimetry and differential thermal analysis (TG-DTA) studies were performed using a Rigaku Thermoplus TG8120. Samples were heated from 300 to 500°C at various heating rates (20, 10, 5 and 2 K min^{-1}) in 150 cm^3 min^{-1} of flowing He. During the thermal analysis, the desorbed substances from the samples were investigated by evolved gas analysis (EGA) using an HP6890 Series gas chromatograph system with a 5973 Mass Selective Detector.

2.3. Analyses

Activation energies of the Hofmann degradation were determined as follows. The DTG-EGA data were applied to the following equation and the values of $\ln(b/T_m^2)$ were plotted versus $1/T_m$, which is the well-known Kissinger plot [16].

$$\ln\left(\frac{b}{T_m^2}\right) = -\frac{E}{RT_m} + \text{constant} \quad (1)$$

where b, T_m, E and R are the heating rate, the absolute temperature at maximum reaction rate, i.e. peak top temperature, the activation energy and the gas constant, respectively. Using this equation, the activation energy can be estimated without assuming a reaction mechanism.

Kinetic analyses of the Hofmann degradation for *n*-OA intercalated Al-AP samples were also carried out by Ozawa's method [17–18]. The TG data were recorded at various heating rates b within a certain temperature range. The start and end of the mass loss were determined from the DTG curves. From the mass loss curves, temperatures T at certain mass loss fraction α value from 0.05 to 0.95, at 0.05 intervals, were obtained, where α is the fraction converted. Using these data, $\log b$ was plotted versus $1/T$ for 19 values of α. The kinetic analyses were carried out using the following equation [19].

$$\log b = -2.315 + \log\left[\frac{AE}{Rg(\alpha)}\right] - \frac{0.4567E}{RT} \quad (2)$$

where b, T, A, E and R are the heating rate, the absolute temperature, the pre-exponential factor, the activation energy and the gas constant, respectively; $g(\alpha)$ is a function of a certain mechanism in the solid state reaction. The designations for rate-controlling process of the mechanisms using in this calculation are listed in Table 2. The above equation is satisfied if parallel straight lines should be obtained. E is then calculated from the linear relation in the α range of 0.15–0.85. The averaged value is used for the following calculations.

Table 2
Designations of rate-controlling process

Designation	Rate-controlling process
F1	Random nucleation, one nucleus on each particle
A2	Random nucleation, Avrami Eq. (1)
R2	Phase boundary reaction, cylindrical symmetry
D2	Two-dimensional dispersion, cylindrical symmetry
D4	Three-dimensional dispersion, spherical symmetry

The reaction mechanism is then obtained. At first, the reduced time θ introduced by Ozawa is calculated using the following equation:

$$\log\theta = \log\left(\frac{E_m}{bR}\right) - \left(2.315 + 0.4567\frac{E_m}{RT_e}\right) \quad (3)$$

where E_m is the averaged activation energy obtained above and T_e is temperature when $b = 1\ \text{K min}^{-1}$ determined by extrapolation of $\log b$ versus $1/T$ plots for each α to $\log b = 0$, i.e. the values of θ can be determined for each α. The values of θ were then applied to the equation

$$g(\alpha) = A\theta \quad (4)$$

When the selected reaction mechanism represented by $g(\alpha)$ is correct, a plot of the $g(\alpha)$ versus θ will give a straight line, the slope of which is equal to A, the pre-exponential factor. Selection of correct reaction mechanism is made by comparing the correlation coefficient obtained by the least square method.

3. Results and discussion

3.1. Kinetic analyses using the DTG data

The DTG curves for *n*-OA-treated Al-AP-010 recorded for various heating rates are shown in Fig. 1. During the Hofmann degradation, one distinct peak was observed at ca. 400°C in the DTG curve. Since no shoulder peaks or overlapping peaks were observed, the mass loss process should be the same and independent of heating rate. For other Al-AP samples, a similar thermal behavior is observed in the DTG curves. The peak top temperatures were used for the kinetic analysis. Kissinger plots using these data for each sample showed that straight lines could be drawn by the method of the least squares (for example, the plot for Al-AP-010 shown in Fig. 2).

According to the analyses using the DTG data, activation energies of the Hofmann degradation were estimated within the range of 188.5−201.7 kJ mol^{-1} (Table 3). This value is in good agreement with the value of 213.5 kJ mol^{-1}, which is the activation

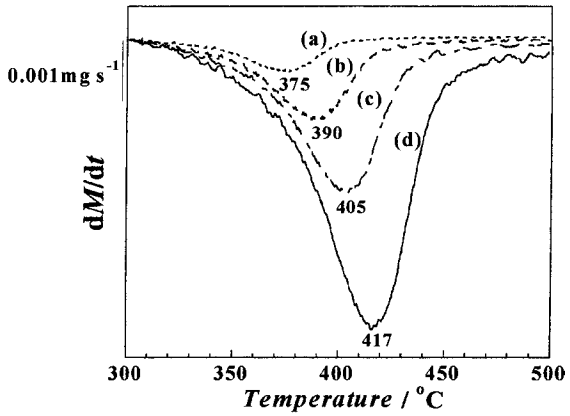

Fig. 1. DTG curves of the Hofmann degradation for *n*-octylamine adsorbed on the sample, Al-AP-010 (Al/Si = 0.17) recorded at (a) 2 K min^{-1}; (b) 5 K min^{-1}; (c) 10 K min^{-1} and (d) 20 K min^{-1}.

energy for the decomposition of *n*-butylamine around 400°C on a silica–alumina sample [4]. The results indicate that the activation energy increase with increasing the Al/Si ratio of Al-AP, see Fig. 3. With respect to the change in acid properties due to the Al/Si ratio, some studies of amine molecules adsorbed on aluminosilicate samples were done by infrared absorption spectrometry [7,15]. They, hence, concluded that the strength of the adsorption site decreases with the amount of increasing Al in the samples since the wave number of the NH_3^+ asymmetric vibration band is reduced with increasing Al/Si ratio. It is assumed that

Table 3
Activation energy of *n*-octylamine decomposition in the Hofmann degradation obtained by Kissinger plot

Sample	Al/Si ratio	Activation energy (kJ mol^{-1})		
		DTG	EGA (1-octene)	EGA (ammonia)
Al-AP-100	0.05	188.5	201.0	207.5
Al-AP-050	0.09	188.9	177.6	181.8
Al-AP-020	0.13	191.8	193.4	180.9
Al-AP-010	0.17	201.7	196.2	182.8
Al-AP-005	0.18	199.6	201.4	171.7

the Hofmann degradation would occur at Brønsted acidic site generated by Al on aluminosilcate sheet. The trend of the activation energy may be associates with the acid strength of Al-AP; strong acid sites would function to lower the activation energy of decomposition.

3.2. Kinetic analyses using the EGA data

Every EGA curve of both 1-octene ($m/z = 112$) and ammonia ($m/z = 17$) simultaneously recorded with the DTG curves have one evolution peak around 400°C, where *m/z* is a number of mass/charge ratio of the molecular ion. In Fig. 4, the EGA curves of 1-octene and ammonia from Al-AP-010 recorded at various heating rates are shown as an example. From Kissinger plots of both 1-octene and ammonia,

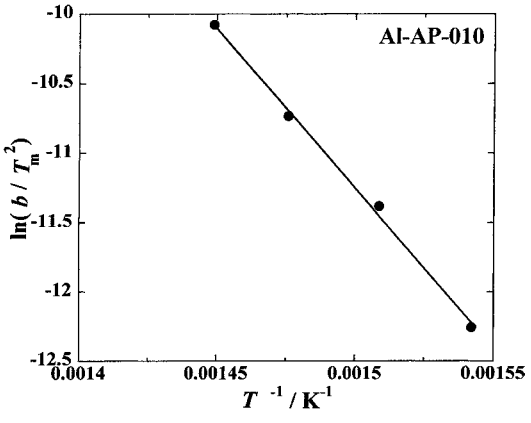

Fig. 2. Kissinger plot of the Hofmann degradation for *n*-octylamine adsorbed on the sample, Al-AP-010 (Al/Si = 0.17) using DTG data.

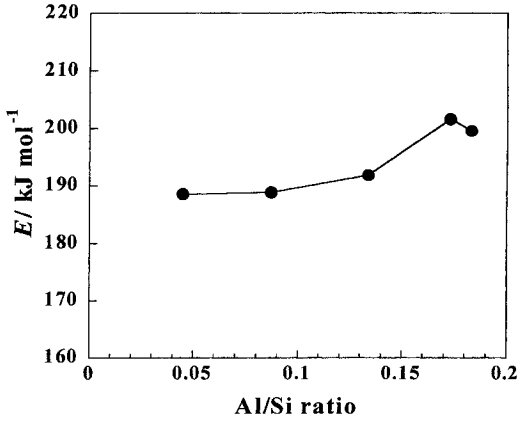

Fig. 3. Relationship between activation energy of the Hofmann degradation obtained using DTG data and Al/Si ratio of Al-AP samples.

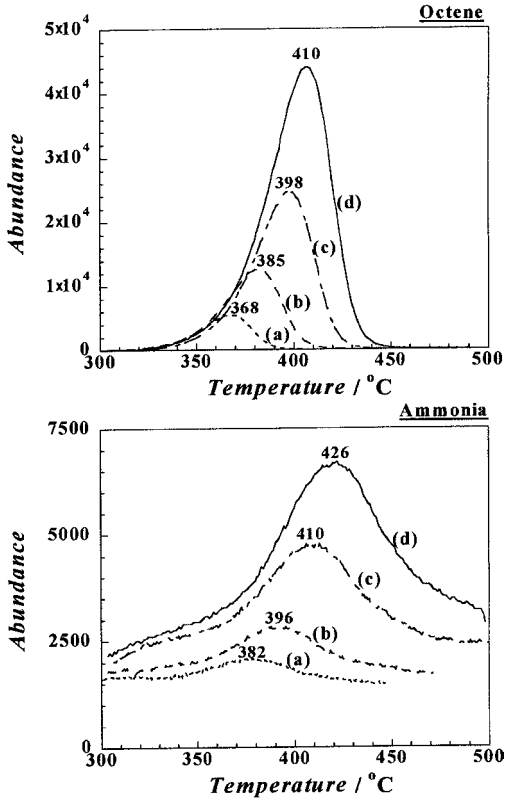

Fig. 4. EGA curves of 1-octene and ammonia evolved in the Hofmann degradation for *n*-octylamine adsorbed on the sample, Al-AP-010 (Al/Si = 0.17) recorded at (a) 2 K min^{-1}; (b) 5 K min^{-1}; (c) 10 K min^{-1} and (d) 20 K min^{-1}.

straight lines drawn by the method of the least square showed good linearity for each sample (for example, the plots for Al-AP-010 shown in Fig. 5).

From the slope of the lines, the activation energies of the Hofmann degradation were obtained in the range 171.7−207.5 kJ mol^{-1} for both 1-octene and ammonia (Table 3), and they were similar to the results from the DTG data. However, relationships between the activation energies obtained for evolved 1-octene and ammonia and the Al/Si ratio of the aluminosilicate showed different tendency. The activation energies estimated from the EGA curves of 1-octene seem to be increasing with the Al/Si ratio except for Al-AP-100. This tendency was analogous to that of the plot for the DTG data, though it has some exception.

From the EGA data of ammonia and 1-octene, the activation energy of ammonia does not depend on the

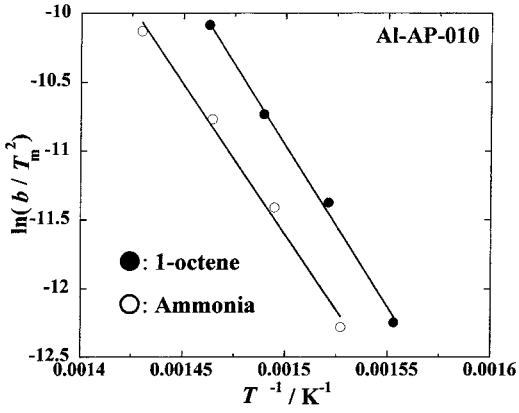

Fig. 5. Kissinger plot of the Hofmann degradation for *n*-octylamine adsorbed on the sample, Al-AP-010 (Al/Si = 0.17) using EGA data of 1-octene and ammonia.

Al/Si ratio above 0.09, see Fig. 6. Thus it appears that the desorption process of ammonia is different from that of 1-octene for higher Al/Si ratios of Al-AP. There is no evolution peak above ca. 400°C on the EGA curves of ammonia in this study. Hence, re-adsorption of ammonia [20] does not occur. It is assumed that the released basic ammonia have some interaction with the the acidic sites of Al-AP surface. Hence, it is assumed that ammonia still remain on the sample surface after the decomposition. Hence, the values of the activation energies obtained for ammonia correspond to the acid strength of the Al-AP samples and not to decomposition of *n*-octylamine.

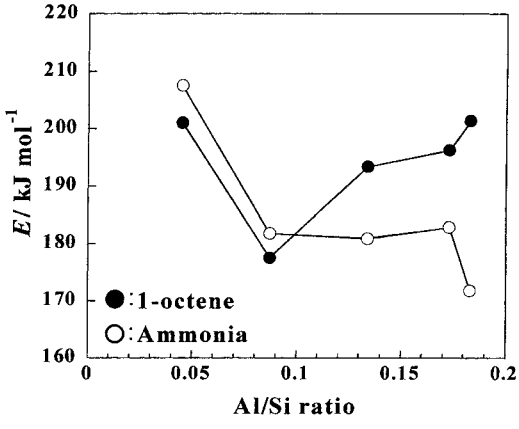

Fig. 6. Plots of activation energy of the Hofmann degradation obtained by Kissingeer plot using EGA data of 1-octene and ammonia as a function for Al/Si ratio of Al-AP samples.

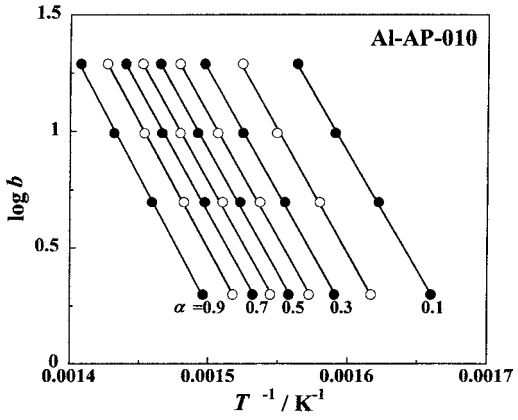

Fig. 7. Ozawa plots of log v vs. T^{-1} for different α of the Hofmann degradation of n-octylamine on the sample, Al-AP-010 (Al/Si = 0.17).

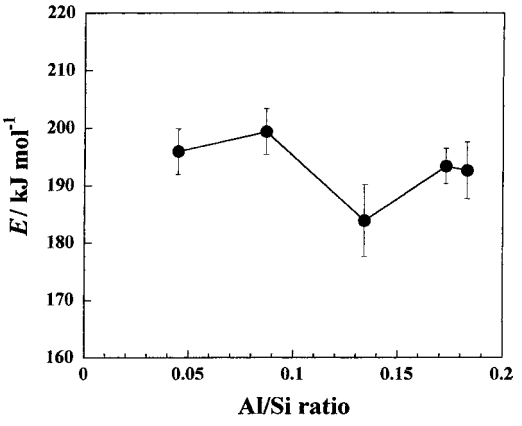

Fig. 8. Relationship between activation energy of the Hofmann degradation obtained by Ozawa's method and Al/Si ratio of Al-AP samples.

3.3. Kinetic analyses by Ozawa's method

Plots of log b versus $1/T$ for different α (using data obtained from n-OA treated Al-AP-010) values are shown in Fig. 7. The parallel straight lines are obtained over almost the entire range of α, especially in the range of 0.2−0.8 for all samples. This indicates that the reaction at ca. 400°C could be treated as a single elementary reaction and the activation energies E_m of the Hofmann degradation could be estimated from the slope of each line. Similar operations were done for data of all samples since parallel straight lines were obtained. The averaged E_m values are listed in Table 4 and the relationship with the Al/Si ratio of the Al-AP is shown in Fig. 8. The result shows good agreement with the E_m values obtained from the DTG data in the same range of 180−200 kJ mol^{-1}. In addition, the activation energy seems to be independent of Al/Si ratio. The reason for the results can be postulated that the decomposition of n-octylamine observed on the Al-AP samples should not be a single elementary reaction and it causes the relationship in Fig. 8 to be complex.

Plots of $g(\alpha)$ versus θ were made for all samples. From the plot for Al-AP-010 (Fig. 9), linearity is best when assuming a reaction mechanism of D2. With a relatively high Al/Si ratio (0.13−0.18), the same tendency was observed and it suggested that D2 should be the correct mechanism. However, for the sample with a lower Al/Si ratio (under 1.00), the linearity of the D2 plot was not as good as that of the D4 plot. These results indicate that the decomposition mechanism of n-octylamine would depend on the Al/Si ratio of the samples.

From the TG data, amount of n-OA decomposing around 400°C was larger for the sample with a relatively higher Al/Si ratio [15]. This means that considerable amount of n-OA remains between the

Table 4
Results of kinetic analyses by Ozawa's method for n-octylamine decomposition in the Hofmann degradation

Sample	Al/Si ratio	Activation energy (kJ mol^{-1})	A (s^{-1})	Reaction mechanism (R^a)
Al-AP-100	0.05	195.9 ± 4.9	6.72×10^{12}	D2 (0.999)
Al-AP-050	0.09	199.4 ± 3.1	1.22×10^{13}	D2 (0.999)
Al-AP-020	0.13	183.9 ± 6.3	2.06×10^{12}	D2 (0.998)
Al-AP-010	0.17	193.4 ± 4.0	4.19×10^{11}	D4 (0.999)
Al-AP-005	0.18	192.6 ± 4.0	3.91×10^{12}	D4 (0.999)

[a] Correlation coefficient.

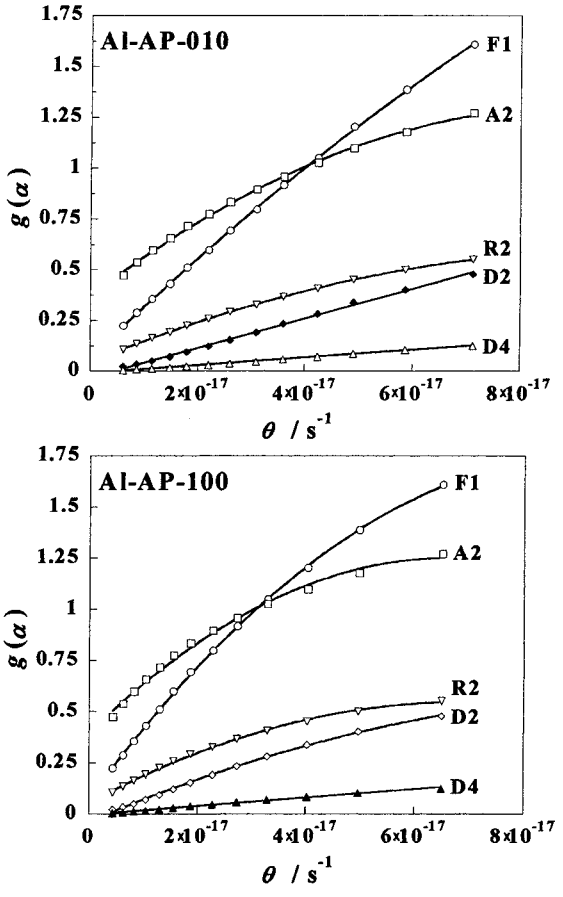

Fig. 9. $g(\alpha)$ vs. θ plots of the Hofmann degradation of *n*-octylamine on the sample, Al-AP-010 (Al/Si = 0.17) and Al-AP-100 (Al/Si = 0.05) for various kinetic mechanisms.

aluminosilicate sheets for the higher Al/Si ratio samples until the Hofmann degradation. With respect to these results, the following schematic drawings are believed to illustrate the processes for *n*-octylamine decomposition in an Al-AP sample. For samples with a high Al/Si ratio (Fig. 10), the interlayer distance is assumed to have little change during decomposition. This indicates that the gas evolved due to decomposition could mainly move in the two-dimensional direction along the aluminosilicate sheets. This assumption explains the results of the analyses. On the other hand, the sample with a relatively lower Al/Si ratio showed that it retains a smaller amount of *n*-OA after desorption under 300°C that narrows its interlayer space and the evolved gas could not move smoothly through

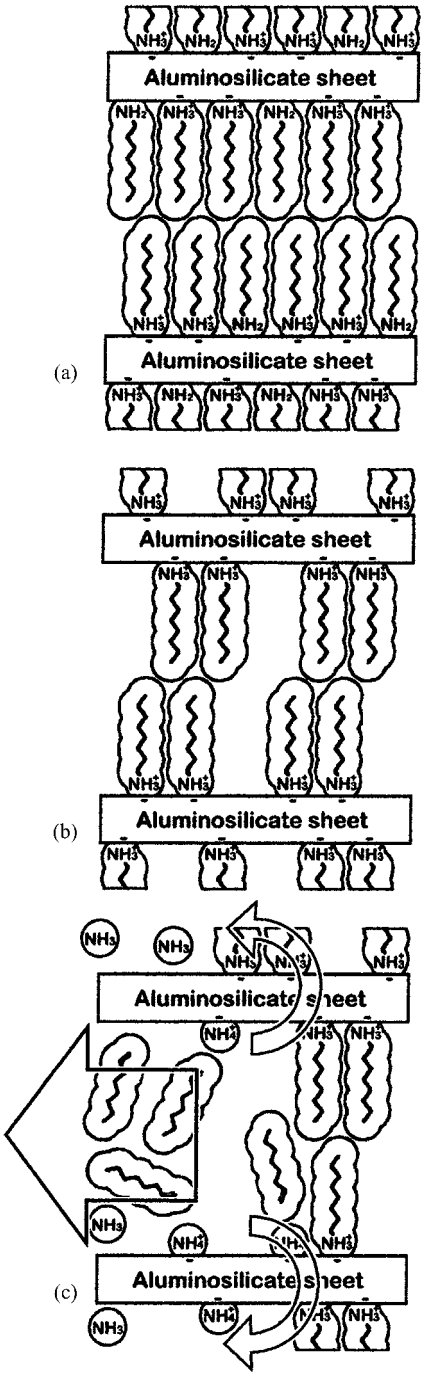

Fig. 10. Schematic drawings for the Hofmann degradation of *n*-octylamine on layered aluminosilicate sample with relatively high Al/Si ratio: (a) before heating; (b) until 350°C and (c) around 400°C.

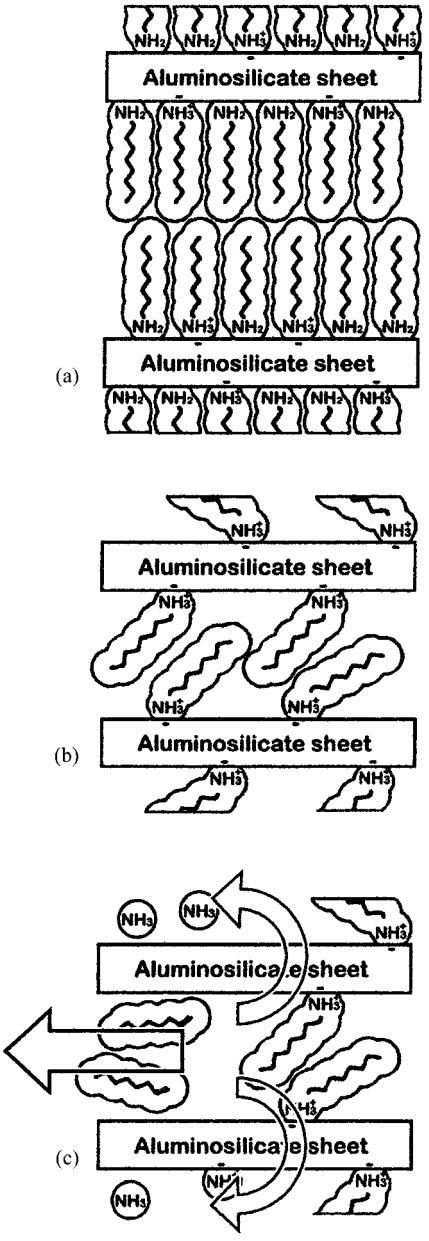

Fig. 11. Schematic drawings for the Hofmann degradation of *n*-octylamine on layered aluminosilicate sample with relatively low Al/Si ratio: (a) before heating; (b) until 350°C and (c) around 400°C.

the interlayer, see Fig. 11. Hence the amount of evolved gas through the eight-membered rings of the SiO_4 tetrahedra in the aluminosilicate sheet becomes relatively larger to that through the interlayer. Due to this, a three-dimensional dispersion (D4) would be valid reaction mechanism for the sample with relatively lower Al/Si ratio. The above interpretation seems to be valid since the schematic models are good agreement with the results of the analyses.

4. Conclusion

The activation energies for the Hofmann degradation of *n*-OA on aluminosilicates prepared from apophyllite were obtained in the range of 180−200 kJ mol^{-1}. According to the kinetic analyses using a Kissinger plot, larger activation energy is observed for the decomposition of *n*-octylamine adsorbed on the higher Al/Si samples than the lower ones. This tendency corresponds to the results of the infrared absorption spectra that showed the sample with a higher Al/Si ratio does not have a very strong acidity. On the other hand, results of the kinetic analyses by Ozawa's method showed no tendency in the plot of the Al/Si ratio versus the activation energy. This indicates that the real reaction process is not a single one but a more complex reaction though the TG data could be treated as a single elementary reaction for the analyses. The reaction mechanism of the Hofmann degradation on the aluminosilicates was basically a two-dimensional dispersion (D2), however, a three-dimensional dispersion (D4) for the relatively lower Al/Si samples. These are suitable results for the reaction models of the aluminosilicate — *n*-octylamine complex.

Acknowledgements

This study was partially supported by grant-in-aid of MESC Japan (No. 09501034) and a Waseda University Grant for Special Research projects (99A-183).

References

[1] C. Frondel, Am. Mineral 64 (1979) 799.
[2] G. Lagaly, K. Matouschek, N. J. Mineral Abh. 138 (1980) 81.
[3] Y. Sogo, F. Iizuka, A. Yamazaki, J. Ceram. Soc. Jpn. 106 (1998) 160.

[4] J.M. Guil, J.E. Herrero, A.R. Paniego, J. Colloid Interface Sci. 102 (1984) 111.
[5] P.A. Jacobs, J.B. Uytterhoeven, J. Catal. 26 (1972) 175.
[6] P.A. Jacobs, B.K.G. Theng, J.B. Uytterhoeven, J. Catal. 26 (1972) 190.
[7] T. Morimoto, J. Imai, M. Nagao, J. Phys. Chem. 78 (1974) 704.
[8] U. Shuali, L. Bram, M. Steinberg, S. Yariv, Thermochim. Acta 148 (1989) 445.
[9] C. Breen, Clay Mineral 26 (1991) 473.
[10] A.K. Ghosh, G. Curthoys, J. Phys. Chem. 88 (1984) 1130.
[11] A.K. Ghosh, J. Catal. 96 (1985) 288.
[12] L.M. Parker, D.M. Bibby, R.H. Meinhold, Zeolites 5 (1985) 384.
[13] U. Shuali, M. Steinberg, S. Yariv, M. Müller-Vonmoos, G. Kahr, A. Rub, Clay Mineral 25 (1990) 107.
[14] H.H.P. Yiu, D.R. Brown, P.A. Barnes, Catal. Lett. 59 (1999) 207.
[15] Y. Sogo, T. Kumazawa, K. Okihara, A. Yamazaki, Extended Abstract Book of the 35th Japanese Conference on Calorimetry and Thermal Analysis, 1999, p. 126.
[16] H. Kambe, T. Ozawa, Netsu Bunseki, Kodansha, Tokyo, 1992.
[17] T. Ozawa, Bull. Chem. Soc. Jpn. 38 (1965) 1881.
[18] T. Ozawa, J. Them. Anal. 2 (1970) 301.
[19] H. Tanaka, Shimazu Kagaku Keisoku J. 3 (4) (1991) 420.
[20] H. Kosslick, G. Lischke, B. Parlitz, W. Storek, R. Fricke, Appl. Catal. A 184 (1999) 49.